in: Rare-Earth-Doped Devices (Photonics West '97), Seppo Honkanen, Ed., Proc. of SPIE, Vol. 2996, 1997, p. 154

Er-doped $LiNbO_3$ waveguide lasers

W. Sohler and H. Suche

Universität-GH Paderborn, Angewandte Physik
Warburgerstraße 100, D-33098 Paderborn, Germany

ABSTRACT

The state-of-the-art of Er-doped integrated optical lasers in $LiNbO_3$ is reviewed. They are fabricated in Er-diffusion doped substrates with Ti-diffused channel guides of high quality. The laser resonators are formed by dielectric mirrors vacuum-deposited on the polished waveguide end faces. Five different types of Ti:Er:$LiNbO_3$ waveguide lasers are presented. Among them are free running Fabry-Perot lasers of six different wavelengths in the range $1530nm < \lambda < 1610nm$ with a cw-output power up to 63mW. They have a shot noise limited relative intensity noise (RIN) at frequencies above 50MHz. Tunable lasers have been developed by the intracavity integration of an acoustooptical amplifying wavelength filter yielding a tuning range up to 31nm. With an intracavity electrooptic phase modulator modelocked laser operation has been obtained with pulse repetition frequencies up to 10GHz; pulses of only a few ps width could be generated. With an intracavity amplitude modulator Q-switched laser operation has been achieved with of up to 2.4W pulse peak power (0.18μJ) at 2kHz repetition frequency. Moreover, distributed Bragg reflector (DBR-) lasers of emission linewidth < 8kHz have been developed using a dry-etched surface grating as one of the mirrors of the laser cavity.

Keywords: $LiNbO_3$, integrated optics, Er-doping, optical amplification, waveguide lasers, tuning, pulse generation, monolithic integration

1. INTRODUCTION

In the last few years the success of the Er-doped fiber amplifier (EDFA) for applications in optical communications (third telecommunication window) has also stimulated a growing interest in Er-doped integrated optical devices, especially lasers. Among the different possible substrates for Er-doped waveguide lasers $LiNbO_3$ is very attractive [1, 2]. In contrast to vitrious and many other crystalline materials $LiNbO_3$ allows the incorporation of Er up to the solid solubility limit without fluorescence quenching [3]. Moreover, due to its excellent electrooptic and acoustooptic properties it allows to develop devices of higher functionality by monolithic integration of intra- and extracavity electrooptical and acoustooptical components. These features promise waveguide lasers of high power conversion efficiency, wavelength tunability over tens of nanometers, Q-switched pulse generation of high peak power, modelocked pulse generation in the GHz range and even the monolithic integration of waveguide lasers with other active and passive components to form application specific integrated optical circuits (ASOC's) of higher complexity.

In this paper the state-of-the-art of Er-doped integrated optical lasers in $LiNbO_3$ is reviewed. In section 2 the fabrication and properties of Er-doped waveguides will be briefly discussed. In section 3 the different types of lasers realized to date are reviewed. In subsection 3.1 a highly efficient free running Fabry Perot laser will be presented. In subsection 3.2 the development of acoustically tunable lasers is reported. Modelocked and Q-switched lasers are discussed in subsections 3.3 and 3.4. A suitable laser for monolithic integration with other devices is a DBR-laser. The properties of such a laser will be described in section 3.5. Finally, concluding remarks will be given together with some ideas for the realization of monolithic ASOC's in the future.

2. ER-DOPED WAVEGUIDES

In principle there are two ways to fabricate Er-doped waveguides in $LiNbO_3$: homogeneously-doped or surface-doped crystalline wafers can be used as waveguide substrate. Homogeneous doping can be achieved during crystal growth from an Er-doped melt [4]. However, it is difficult to achieve high

quality striation-free crystals of high doping concentration and large size. The introduction of rare earth ions tends to increase the number of domains in the crystal [5].

On the other hand, Er-doping of a surface layer as alternative can be achieved by implantation and annealing [6] or by indiffusion of vacuum-deposited Er-layers [1, 2, 7]. For the surface-doping techniques commercially available $LiNbO_3$-wafers of high optical quality and large diameter can be used. The diffusion doping is easier to apply and produces waveguides of higher quality (less up-conversion and lower scattering loss) than implantation doping. It is ideally suited for a selective doping of the surface using photolithographic patterning of the evaporated Er- or Er_2O_3-layers, respectively. This selective doping is a prerequisite for the monolithic integration of active (optically pumped, Er-doped) and passive (unpumped) devices on the same substrate to avoid reabsorption in unpumped Er-doped waveguide sections.

The process of Er-indiffusion has been characterized in detail using Secondary Ion Mass Spectroscopy (SIMS), Secondary Neutral Mass Spectroscopy (SNMS), Rutherford Backscattering Spectroscopy (RBS), and Atomic Force Microscopy (AFM) [7]. The site of the Er^{3+}-ions in the $LiNbO_3$-lattice has been determined using X-ray Standing Wave Spectroscopy (XSW) [8] and Optical Site Selective Spectroscopy (OSSS) [9].

The diffusion of erbium into $LiNbO_3$ can be described by Fick's laws with a concentration-independent diffusion coefficient and a temperature-dependent maximum solubility [7]. Typical Er-doping profiles before and after the fabrication of a planar Ti-indiffused waveguide in a Z-cut $LiNbO_3$ substrate are shown in Fig. 1 together with the Ti-profile.

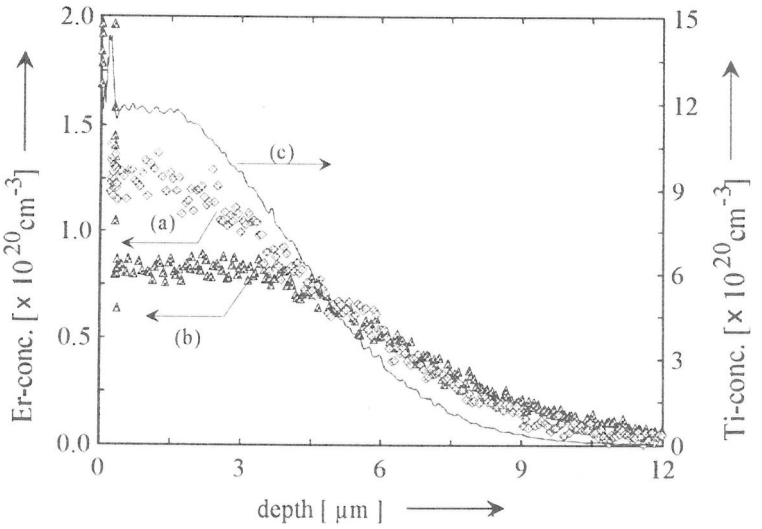

Fig. 1: Erbium and titanium concentrations versus depth in a Z-cut $LiNbO_3$ wafer measured by SNMS (Er) and SIMS (Ti), respectively. Er-profile after indiffusion of a 22nm thick Er-layer at 1130°C within 100h (a). Er-profile after additional indiffusion of a 95nm thick Ti-layer at 1030°C within 9,h (b). Corresponding Ti-distribution (c).

Due to the anisotropic crystal structure of $LiNbO_3$ the diffusion coefficient of Er in $LiNbO_3$ depends on the crystal cut with the highest diffusivity along the crystal Z-axis [7]. It is about two orders of magnitude smaller than that of titanium. Therefore, the Er-diffusion-doping has to be performed prior to the waveguide fabrication. To achieve a good overlap of the doping profile and the optical waveguide modes the Er-diffusion has to be performed at a temperature as high as possible and close to the Curie-temperature of ferroelectric $LiNbO_3$ (1142°C for congruent melting material [10]) for at least 100h. The solubility of erbium (about $1.7\times10^{20}cm^{-3}$ at 1100°C) is about one order of magnitude smaller than that of titanium; it grows exponentially with the temperature [7].

During indiffusion of a vacuum-deposited Er-layer the surface concentration of the dopant corresponds to the solubility level as long as the diffusion reservoir is not exhausted. Afterwards the concentration drops according to Fick's laws. To prevent the formation of precipitates of Er_xNb_y-oxide compounds

during the waveguide fabrication the Er-surface concentration should be at least slightly below the solid solubility level at the waveguide fabrication temperature.

Er is incorporated into $LiNbO_3$ on a vacant Li-site or replaces lithium [8]. Site-selective spectroscopy found four slightly different erbium sites [9]. This has been attributed to perturbations of the local crystal field due to variations of the arrangement of charge compensating defects.

Up to now Er-doped waveguides of very low scattering losses could only be fabricated by Ti-indiffusion into the Er-doped $LiNbO_3$ surface; scattering losses below 0.1dB/cm have been measured in doped Ti-diffused waveguides with an Er-surface concentration up to $5\times10^{19}cm^{-3}$.

By optical pumping of such a waveguide up to 13.8dB net single pass small signal gain (fiber to fiber) has been achieved [11].

The proton-exchange technique gave waveguides of lower quality. The fluorescence yield of the $^4I_{13/2} \rightarrow {}^4I_{15/2}$ transition is very low and the scattering losses of Er-diffusion doped, annealed and proton exchanged waveguides could not be reduced below 1dB/cm. [12].

3. WAVEGUIDE LASERS

Waveguide amplifiers are the basic devices to develop integrated lasers. Incorporated in an optical cavity to achieve the necessary feedback laser oscillation can be obtained above a certain threshold by sufficient optical pumping. The simplest laser is a free running (without intracavity control elements) laser with a Fabry Perot cavity. It has the lowest intracavity losses, and therefore, the potential for a high power conversion efficiency. Such a device of optimized efficiency will be presented in the following subsection. More advanced lasers can be developed by integrating a modulator or (and) a wavelength filter in the waveguide resonator. In this way an intracavity amplifying acoustooptical filter leads to tunable laser operation; a corresponding device is presented in subsection 3.2. An intracavity phase modulator allows to obtain modelocked laser operation and therefore the generation of ultrashort pulses. This is discussed in subsection 3.3. An intracavity amplitude modulator offers the possibility to operate the laser in a Q-switched mode and in this way to generate short pulses of high peak power. Such a Q-switched laser is presented in subsection 3.4. All these different types of lasers are of the Fabry Perot type with a cavity comprised of dielectric mirrors, directly deposited on the polished waveguide end faces. The rear mirror has a high reflectivity at both, the signal- and the pump wavelength to provide double-pass pumping and in this way an improved pump absorption efficiency.

If one of the broadband dielectric mirrors (or even both) is replaced by a Bragg-grating, etched into the surface of the waveguide amplifier the narrow-band reflectivity of this mirror precisely determines the emission wavelength of the laser. Moreover, such a distributed Bragg-reflector-(DBR-) laser, which is described in subsection 3.5, facilitates the monolithic integration of the laser with further devices on the same substrate.

3.1 FREE RUNNING FABRY PEROT LASERS

In a Fabry-Perot type laser without any wavelength-controlling intracavity elements the emission wavelength is determined by the spectral properties of the cavity (wavelength-dependent mirror reflectivities and waveguide scattering losses) and the amplifier gain spectrum. Laser oscillation sets in at the wavelength where the threshold gain is lowest. By a proper choice of the output coupler laser emission at the different maxima of the Er: $LiNbO_3$-gain spectrum can be achieved. Up to now lasers of six different wavelengths have been fabricated: λ_s = 1531nm, 1546nm, 1562nm, 1576nm, 1602nm and 1611nm [13-16].

However, it is a problem to design the cavity in such a way that the maximum quantum efficiency is obtained at any of these wavelengths . In any case, the waveguide amplifier should have low scattering losses and a high absorption efficiency; both can be achieved by an optimized Er-doping profile, an optimized waveguide length and a double-pass pumping scheme. All the waveguide and amplifier parameters then determine the optimum output coupler. Following these guidelines, a laser of optimized efficiency has been recently demonstrated [11]. It has a highly Er-doped straight Ti-diffused channel guide of 7cm length with a small signal gain of up to 13.8dB achieved with a coupled pump power of

190mW. The output coupler of 30% maximum reflectance within the Er-gain bandwidth (70% minimum output coupling efficiency) guarantees that laser oscillation sets in at λ_s = 1562nm with highest quantum efficiency. A maximum output power of 63mW at an incident pump power level of 210mW (color center laser as pump source) has been obtained (see Fig. 2).

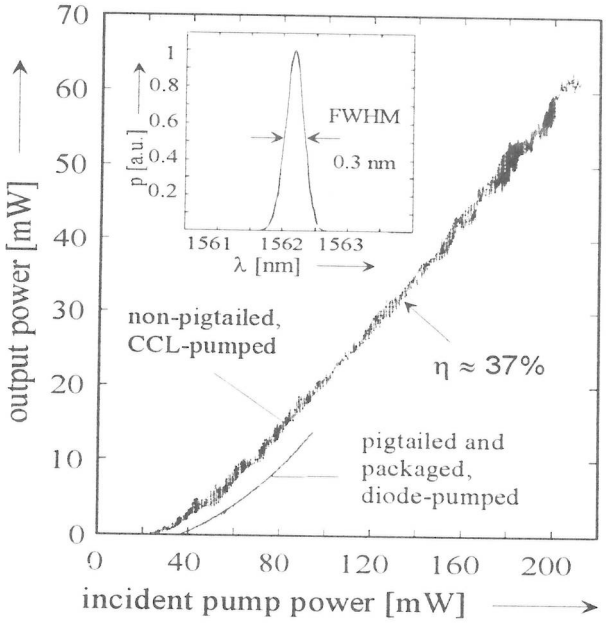

Fig. 2: Output power of a diode-pumped, pigtailed and packaged Ti:Er:$LiNbO_3$ waveguide laser of optimized efficiency versus incident pump power. Both, pump and signal polarization are TE (σ). For comparison the power characteristics of the color center laser- (CCL-) pumped waveguide laser without pigtails is given. Inset: emission spectrum of the diode pumped (95mW) waveguide laser.

The lasing threshold was only 24mW. A slope efficiency up to 37% has been observed. These experimental results are in good agreement with the theoretical predictions. The waveguide laser has been pigtailed, packaged and characterized again using diode-pumping at about 1480nm wavelength. The result is shown in the lower graph of Fig. 2. Only a slight increase of the threshold and a slight decrease of the output power was caused by the pigtailing. A maximum output power of 14mW with strongly reduced noise was achieved at a pump power level of 95mW. Moreover, spectral noise measurements showed that at frequencies above 50MHz the laser output is shot noise limited, while at low frequencies around 350kHz residual relaxation oscillations are observed. They can be drastically suppressed by a feedback controlled pumping.

A further improvement of the laser efficiency seems to be possible. Theoretical calculations predict, that a reduction of the scattering losses from 0.18dB/cm (actual sample) down to 0.08dB/cm would increase the maximum slope efficiency by more than 10% [11]. A higher Er-doping level and improved overlap of the doping profile and the waveguide modes would increase the output power further.

3.2 ACOUSTOOPTICALLY TUNABLE LASER

Tunable lasers are very attractive for a number of applications, such as for wavelength devision multiplexed optical communications or for spectroscopy. In Er:$LiNbO_3$ waveguide lasers high performance acoustooptically tunable wavelengths filters [17] can be used as intracavity devices to provide the required tuning element. The first amplifying filter has been demonstrated in 1994 [18]. But such a single stage filter with external polarizer can not be used for narrow linewidth tunable laser operation. Each stage of acoustooptic mode conversion resp. -filtering is accompanied by a frequency shift of the acoustic frequency. Therefore, a double stage filter respectively a single stage filter with additional shift compensating second mode converter and with integrated polarizers is needed [19]. A tunable laser based on the latter concept has been reported in 1994 [20]. Polarization filtering was provided by a polarization splitter operated as TM-pass polarizer and by a TE-pass polarizer. In the

meantime the laser design has been modified to reduce the intracavity losses and in this way to improve significantly the output power and the tuning range. This laser is discussed below in more detail.

The structure of this more advanced device is shown schematically in Fig. 3. The main difference to the old design described in [20] is the replacement of the TE-pass polarizer by a more stable and less lossy polarization splitter. Moreover, the Er-doping and waveguide fabrication have been optimized to give a better pump absorption efficiency, higher signal gain and lower scattering losses.

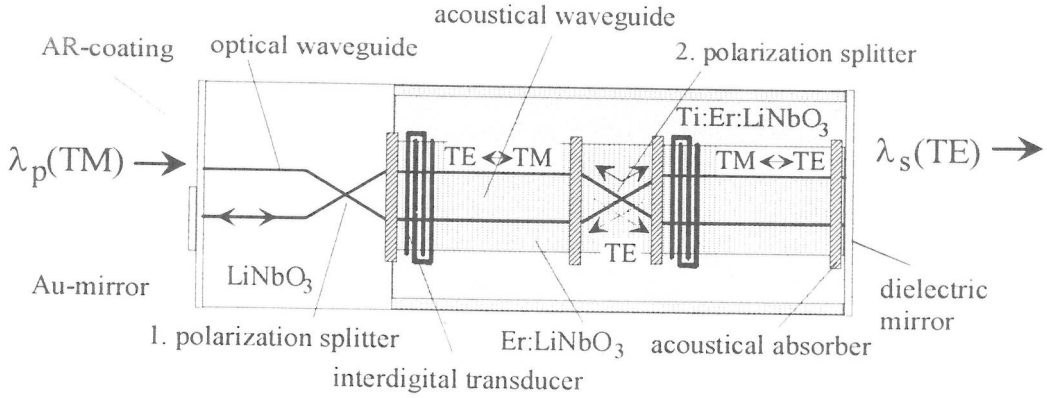

Fig. 3: Schematical sketch of the improved acoustooptically tunable Ti:Er:$LiNbO_3$-waveguide laser; the routing of the converted and unconverted signal light is indicated for polarization dependent operation; the total device length is 63mm.

The polarization-dependent routing is indicated for a TM-polarized pump mode and a signal mode that is TE-polarized at the mirrors of the laser cavity (polarization-dependent operation). Starting from the left cavity mirror the TE-polarized signal is routed cross by the first polarization splitter and superimposed to the TM-polarized pump which travels along the upper branch of the waveguide structure. Only the phase-matched part of the signal is converted (wavelength selective) by the first acoustooptical mode converter to TM and passes -- together with the pump mode -- the right polarization splitter in the bar state. The unconverted part of the TE-polarized signal is directed cross to the unpumped lower branch of the right mode converter and is hence absorbed. The already once-filtered TM-polarized signal light is converted back to TE in the second mode converter and then fed back by the right cavity mirror. This broadband dielectric mirror of about 98% reflectance acts as the output coupler for the signal and provides double pass pumping. The left polarization splitter is used as polarization filter and pump coupler, simultaneously. Therefore, a simple Au-layer can be used as the left cavity mirror. Reduced scattering losses of the waveguides - 0.1dB/cm for TE-polarized light and 0.05dB/cm for TM-polarization - and low insertion losses of the other intracavity components resulted in a total cavity round trip loss of ≈ 4.8dB. The bandwidth of the filter of 1.35nm (FWHM) resulted in a laser emission linewidth of about 0.25nm.

The laser has been pigtailed, packaged and characterized using diode-pumping (λ_p=1484nm). The minimum threshold of the packaged device was about 50mW at $\lambda_s \approx$ 1561nm (see power characteristics as inset in Fig. 4). With about 110mW coupled pump power in TM-polarization up to 320μW TE-polarized output power has been measured. The nonlinearity of the power characteristics is attributed to a change of the spectrum of the pump laser diode during the sweep of the injection current. The overall tuning behaviour for diode pumping of the packaged device is shown in Fig. 4. The tuning slope is -8nm/MHz. In the gaps of the tuning characteristics the internal gain was not sufficient to overcome the round trip losses in the laser cavity. However, by using a color center laser as pump source of higher power level a total tuning range of 31nm and continuous tuning from 1540nm to 1568nm was possible.

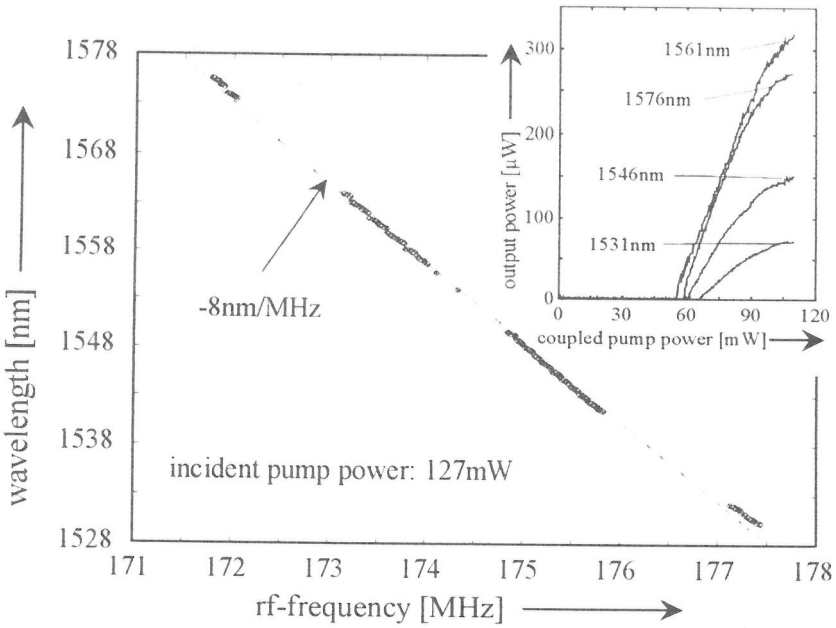

Fig. 4: Emission wavelength versus acoustic frequency of the pigtailed, packaged and diode-pumped acoustooptically tunable Ti:Er:$LiNbO_3$-waveguide laser for 127mW of incident pump power. Inset: power characteristics of the laser for selected wavelengths.

3.3 MODELOCKED LASER

Modelocking is a versatile means to generate pulse trains of high repetition rate and peak power. Therefore, a modelocked laser emitting in the third telecommunication window is regarded as a very promising source for high bitrate soliton-type data transmission. Integrated optical versions of such a modelocked source are rugged and have a high potential for miniaturization. Moreover, sources in electrooptic materials like $LiNbO_3$ allow a monolithic integration of an active modelocker. This has first been demonstrated with Nd: $LiNbO_3$ [21].

With an Er-doped $LiNbO_3$ waveguide laser fundamental and harmonic modelocking have already been reported [15, 16]. As the modelocker a monolithically integrated intracavity phase modulator has been used (FM-type modelocking). However, the output power of these lasers was low and the emission wavelength (1531nm, 1602nm and 1611nm) was not matched to the third telecommunication window due to a non optimized broadband Fabry Perot waveguide cavity.

Recently, a highly efficient harmonically modelocked waveguide laser of suitable emission wavelengths has been demonstrated. The laser is packaged, thermoelectrically temperature controlled and diode-pumped. It has been developed for soliton communication experiments in the European ACTS-project ESTHER (AC063). The structure of this laser together with additional components included in its package is shown schematically in Fig. 5.

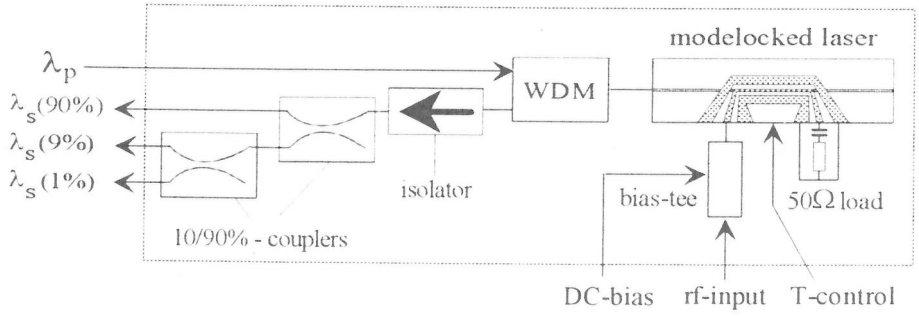

Fig. 5: Schematical structure of the pigtailed and packaged laser, additional components are included in the package for demultiplexing, optical isolation and power splitting.

The Z-cut (Y-propagation) $LiNbO_3$ substrate has been doped near the surface by indiffusion of 28nm of vacuum deposited Er at 1130°C during 125h. Subsequently, photolithographically delineated 7μm wide and 98nm thick Ti-stripes have been indiffused at 1060°C during 8h to form the 66.5mm long low loss waveguide channels. To avoid excess losses of the TM-mode an 0.6μm thick insulating SiO_2-buffer has been vacuum deposited onto the substrate surface prior to the electrode fabrication.

The electrode structure of the modelocker (travelling wave phase modulator) is a symmetrical coplanar microstrip line with a gap to hotline width ratio of 0.75. It has been defined by photolithographic lift off and subsequently electroplated up to a thickness of 4.5μm. By using the waveguide Fabry Perot with intracavity phase modulator as an optical spectrum analyzer [22] a halfwave voltage V_π of 5.4V for TM and 21.6V for TE was measured, respectively.

The laser cavity is comprised of a high reflector on the right side (see Fig. 5) and a pump/signal coupler on the left of optimized output coupling for the signal (see discussion in subsection 3.1). The latter mirror has a minimum reflectivity of about 7% at the pump wavelength ($\lambda \approx 1480$nm) and a transmittance of about 55% at the signal wavelength. A frequency spacing of the axial cavity modes of 994.3MHz for TE- and 1029.5MHz for TM-polarization has been determined from the beat frequency of neighbouring cavity eigenmodes using an electronic spectrum analyzer.

The pump input side of the cavity was pigtailed with the common branch of a fiberoptic wavelength division demultiplexer (WDM) to allow coupling of a pigtailed pump laser diode and extraction of the laser output in backward direction. Finally, the pigtailed laser has been packaged including optical isolation, thermoelectric temperature control ($< \pm 0.01$K) and two cascaded 10/90% power splitters (see Fig. 5). 90% of the laser output can be used for data encoding. The two additional tap outputs (9% , 1%) allow to monitor the modelocking stability and pulse peak power and to derive a control signal for feedback stabilization (controlled pumping).

To pump the modelocked Ti:Er:$LiNbO_3$-waveguide laser a high power laser diode of 1480nm center wavelength and 12nm spectral width has been used. Up to 140mW of incident pump power were available at the common branch of the WDM.

In Fig. 6 the cw-power characteristics of the Er-laser is shown for TM(π)-polarized emission at 1575nm and TE(σ)-polarized emission at 1562nm wavelength, respectively.

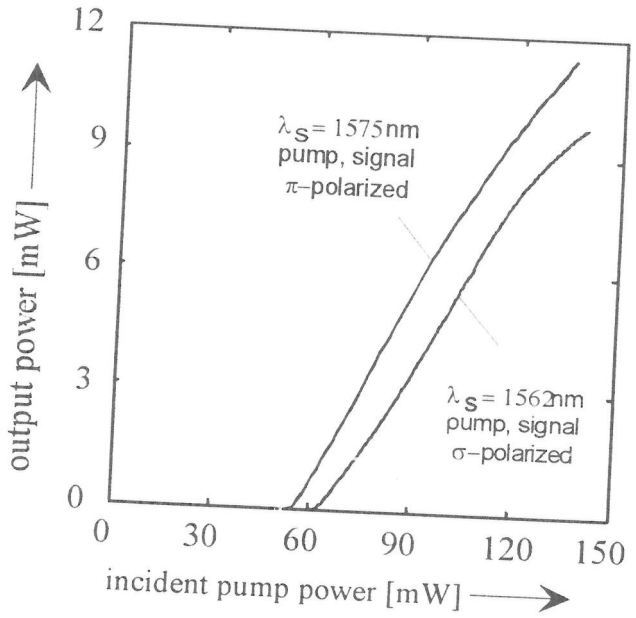

Fig. 6: Output power versus pump power incident at the common branch of the f/o WDM-coupler (see Fig. 5) for both, π- and σ-polarized emission. The polarization dependent emission wavelengths are indicated.

The polarization and wavelength of the emission can be adjusted by the pump polarization. With π(σ)-polarized pumping the Er-laser emits at 1575(1562)nm π(σ)-polarized. Threshold pump power and

slope efficiencies are 56mW(65mW) and 14.4%(13.2%) for π(σ)-polarized emission, respectively. Both, slope efficiency and output power are more than an order of magnitude better than previously reported results [15, 16].

Results of modelocking are shown in Fig. 7, for the 5th harmonic (5.14766GHz) and π-polarized emission at two different levels of the rf-drive power. With 29dBm of rf-power a pulse width of 7.4ps (FWHM) has been determined by deconvolution of the autocorrelation trace assuming a Gaussian pulse shape. Together with the spectral width of 0.77nm a time bandwidth product of 0.68 results. Pulse peak power levels up to 310mW have been achieved. For 16dBm of rf-power the pulse width broadens to about 21ps and the spectral width can be estimated to 0.26nm. However, the stability of the pulses is significantly deteriorated as can be seen from the noise on both, the correlation trace and the spectrum. Modelocking has been observed up to the 10th harmonic at 10.295GHz. For σ-polarized emission at 1562nm wavelength 5th harmonic modelocking has been obtained at 4.97133GHz. Time bandwidth products down to 0.45 have been achieved, but, as a result of the much higher halfwave voltage and the much lower phase modulation index the stability of the pulses was not as good as in the π-polarized case.

Further improvements of the laser seem to be feasible by the development of monolithically integrable low loss Bragg gratings which fix the emission wavelength and allow to tailor the pulse bandwidth and chirp.

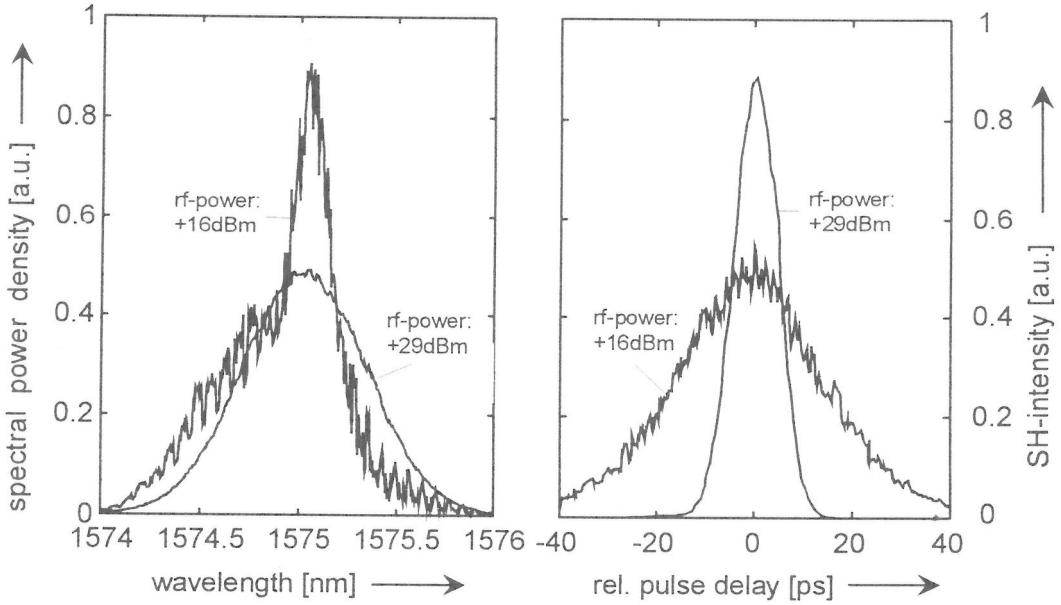

Fig. 7: Modelocking at the 5th harmonic (5.14766 GHz) in π-polarized emission (λ_s = 1575nm); left: spectral power density versus wavelength; right: autocorrelation trace as function of the relative pulse delay; parameter of the set of graphs: incident rf-drive power of the modelocker.

3.4 Q-SWITCHED LASER

An intracavity intensity modulator can be utilized to switch the laser cavity Q-factor. During the low Q-phase the active medium can be pumped to a very high inversion level without exceeding the oscillation threshold. The better the modulator extinction is the more the stored energy in the active medium grows before prelasing sets in. In this way significant excitation energy is stored and can be utilized to generate intense pulses when the cavity is switched back to a high Q. Such a laser utilizing an intracavity Mach-Zehnder type intensity modulator as the Q-switch has been recently demonstrated in a Ti:Er:$LiNbO_3$-waveguide laser [23].

On one side of the waveguide resonator the laser has a dielectric mirror of 98% reflectivity at both, pump- ($\lambda_p \approx$ 1480nm) and emission wavelength ($\lambda_s \approx$ 1561nm). On the other side a variable output/pump coupler mirror has been realized by an adjustable, piezoelectrically driven air gap etalon

formed by the endfaces of the pump input/signal output fiber of a WDM and the polished Ti:Er: $LiNbO_3$-waveguide endface. With diode pumping a threshold of about 58mW has been achieved.

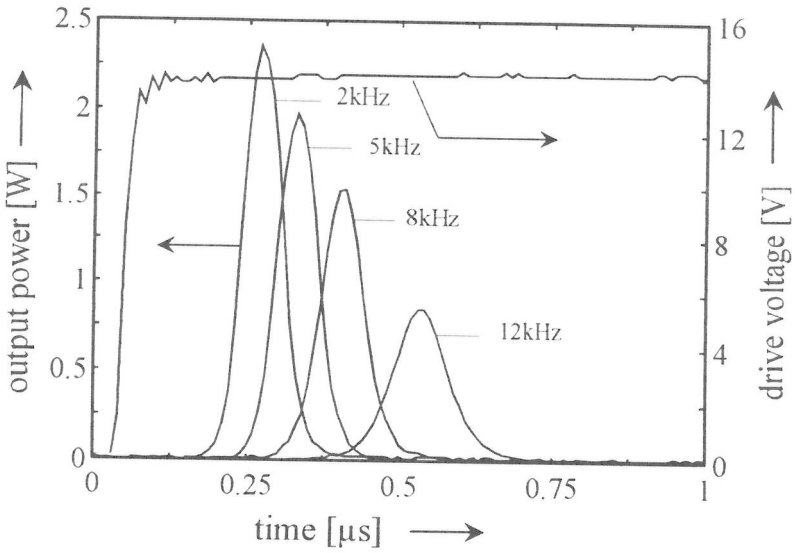

Fig. 8: Output power (left ordinate) and drive signal of the intracavity amplitude modulator (right ordinate) of a Q-switched Ti:Er: $LiNbO_3$-waveguide laser versus time. Parameter is the pulse- or Q-switching repetition frequency.

Using a pigtailed laser diode the Er-laser has been continously pumped with 100mW similar to the scheme shown in Fig. 5. In Fig. 8 first results of Q-switched operation of the Ti:Er: $LiNbO_3$ laser are presented. Both, the drive voltage for the intracavity electrooptic switch and the laser output are shown as function of time. After switching to the high-Q cavity, which corresponds to the zero of the abszissa, pulses of a peak power up to 2.4W and a pulse energy of 0.18µJ are emitted at 2kHz repetition frequency. With increasing frequency the pulses become broader, the peak power is reduced and the pulse build-up-time increases.

Even better result are expected in the future with intracavity switches of higher extinction ratio.

3.5 DBR-LASER

By replacing one of the dielectric endface mirrors of a Fabry-Perot type laser by a (first order) Bragg-grating etched into the surface of Ti:Er: $LiNbO_3$ channel guides DBR-lasers can been fabricated. Their emission wavelength is determined by the periodicity of the grating. Even single frequency operation can be expected in case of a grating response narrower than the frequency spacing of the longitudinal laser modes. With Bragg-gratings of 352nm and 346nm periodicity DBR-lasers for λ_s =1561nm and λ_s =1531nm emission wavelengths have been developed in Z-cut $LiNbO_3$ [24]. It was even possible to fabricate two lasers of both periods on a common substrate. The gratings have been holographically defined in a resist layer and subsequently transferred into the waveguide surface by sophisticated masking and dry etching techniques [25]. The depth of grooves was limited by redeposition effects during etching to about 420nm. The inset in the left diagram of Fig.9 shows an SEM top view of a grating of 352nm periodicity etched 300nm deep into the surface of $LiNbO_3$. In Fig. 9 also the power characteristics (left) and the highly resolved spectrum (right) of one of the 1561nm lasers are shown. The laser has been pigtailed, packaged and temperature-stabilized. Diode-pumping at $\lambda_p \approx$ 1480nm in TE-polarization has been used. At about 45mW pump power laser oscillation sets in. With 110mW pump power about 1.4mW output power has been measured. This poor efficiency is a consequence of the not yet optimized laser cavity with excess losses for pump and signal radiation induced by the grating. Moreover, only single pass pumping is possible with the present design.

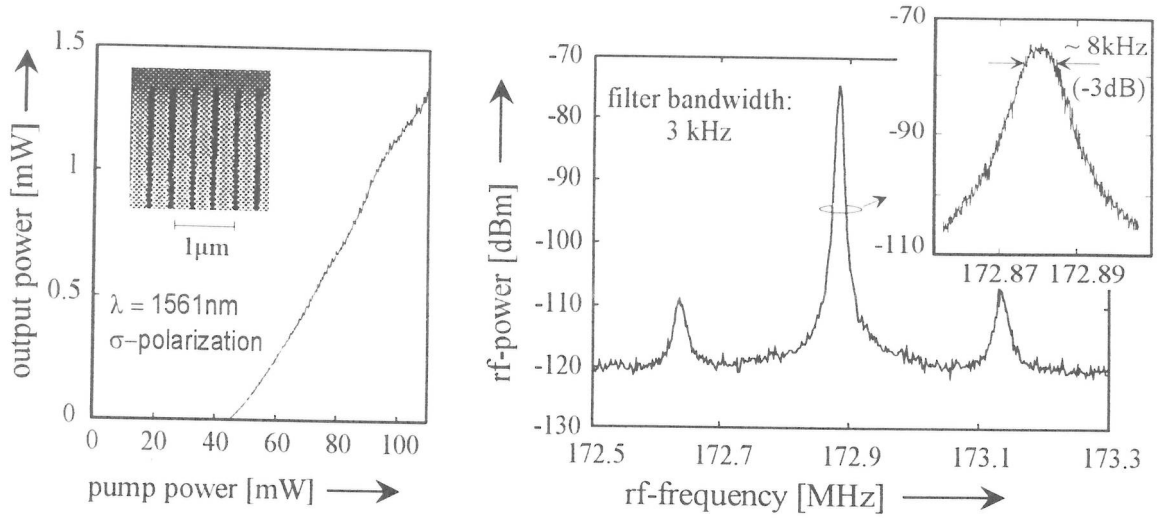

Fig. 9: Power characteristics (left) and self-heterodyne beat spectrum (right) of the emission of a diode-pumped, pigtailed and packaged single frequency DBR-Ti:Er: $LiNbO_3$-waveguide laser. Left inset: SEM-image of the dry-etched first order surface relief grating used as Bragg reflector. Right inset: Peak of the beat spectrum with higher resolution.

The linewidth of the laser emission is very narrow. Using a scanning Fabry-Perot resonator as spectrum analyzer single-frequency operation of the laser could be verified; however, the true linewidth could not be resolved in this way. Therefore, delayed self-heterodyne detection with a 26km long fiber as the delay line in one branch of a fiber optical Mach-Zehnder-interferometer has been used for high resolution spectral analysis. An integrated acoustooptical filter was inserted into the other branch of the interferometer as frequency shifter. The interferometer output was measured and the resulting electronic beat spectrum is shown on the right of Fig. 9. From the 3dB-bandwidth of the spectral power density the laser linewidth can be determined; it is narrower than 8kHz (see right inset of Fig. 9). Feedback controlled pumping and a good optical isolation of the laser output were absolutely necessary.

4. CONCLUSION

Erbium diffusion doping of $LiNbO_3$ allows to develop a variety of different optically pumped integrated laser devices. Besides relatively simple Fabry-Perot-type waveguide lasers more advanced devices of higher functionality can be designed by combining optical amplification and lasing with electro- or acoustooptically controlled functions. Examples are monolithic modelocked, Q-switched and tunable lasers. Furthermore, DBR-lasers are key components for the development of advanced monolithically integrated optical circuits of higher functionality and complexity which combine lasers and other active and passive devices on the same substrate. This new field is of growing interest and open for many ideas to be realized. As a first example an integrated transmitter unit has been recently demonstrated consisting of a narrow linewidth DBR-laser and an extracavity Mach-Zehnder-type encoding modulator on the same Er-doped $LiNbO_3$ substrate [26]. This is a very attractive combination for long-haul fiber optical communications as the extracavity electrooptical waveguide modulator introduces only a negligible wavelength chirp in the laser emission spectrum. Besides laser-modulator combinations (transmitters) more sophisticated circuits are feasible like integrated acoustooptical heterodyne interferometers for optical metrology and vibration analysis with an integrated DBR-laser as highly coherent source and up to 11 additional devices on the same substrate [27]. $LiNbO_3$ is also an excellent nonlinear optical material. Therefore, additional functions can be expected by combining Er-doped DBR-lasers with, e. g. optical parametric frequency converters. In this way, miniaturized all solid state widely tunable coherent sources might become a reality. It is a challenge for the future to design and to develop complex, optically powered, monolithic integrated optics in (selectively) Er-doped $LiNbO_3$ with new application specific optical circuits (ASOC's).

ACKNOWLEDGEMENTS

We gratefully acknowledge the support of this work by the European Union within the RACE-project EDIOLL (R2013), the ACTS-project ESTHER (AC 063) and by the Heinz Nixdorf Institut.

REFERENCES

1. W. Sohler and H. Suche: "RARE-EARTH-DOPED LITHIUM NIOBATE WAVEGUIDE STRUCTURES", European Patent No. 0569353 and U. S. Pat. Appln. Serial No. 08/094,199

2. I. Baumann, R. Brinkmann, Ch. Buchal, M. Dinand, M. Fleuster, H. Holzbrecher, W. Sohler, and H. Suche: "Er-diffused Waveguides in $LiNbO_3$", Proc. European Conf. on Integrated Optics, ECIO'93, paper: 3-14, Neuchatel, 1993

3. M. Fleuster, C. Buchal, E. Snoeks, and A. Polman, "Optical and structural properties of MeV erbium-implanted $LiNbO_3$", J. Appl. Phys., **Vol. 75** (1), pp. 173-180, 1994

4. L. F. Johnson and A. A. Ballman: "Coherent Emission from Rare Earth Ions in Electro-optic Crystals", J. Appl. Phys., **Vol. 40** (1), pp. 297-302, 1969

5. N. F. Evlanova and L. N. Rashkovich: "Domain Structure of Lithium Metaniobate Crystals", Sov. Phys. - Solid State, **Vol. 13** (1), pp. 223-224, 1971

6. R. Brinkmann, Ch. Buchal, St. Mohr, W. Sohler, and H. Suche: "Annealed erbium-implanted single-mode $LiNbO_3$ waveguides", in Technical Digest on Integrated Photonics Research, Optical Society of America, Washington, D.C., 1990 OSA Technical Digest Series, **Vol. 5**, post-deadline paper PD1

7. I. Baumann, L. Beckers, Ch. Buchal, R. Brinkmann, M. Dinand, Th. Gog, H. Holzbrecher, M. Fleuster, M. Materlik, K. H. Müller, H. Paulus, W. Sohler, H. Stolz, W. von der Osten, O. Witte: "Erbium incorporation in $LiNbO_3$ by diffusion-doping", Appl. Phys. A., Vol. 64, pp. 33-44, 1997

8. T. Gog, M. Griebenow, and G. Materlik: "X-ray standing wave determination of the lattice location of Er diffused into $LiNbO_3$", Phys. Lett. A, **Vol. 181** (5), pp. 417-420, 1993

9. O. Witte, H. Stolz, and W. von der Osten: "Upconversion and site-selective spectroscopy in erbium-doped $LiNbO_3$", J. Phys. D: Appl. Phys., **Vol. 29**, pp. 561-568, 1996

10. P. F. Bordui, R. G. Norwood, C. D. Bird, and G. D. Calvert: "Compositional uniformity in growth and poling of large-diameter lithium niobate crystals", J. Crystal Growth, **Vol. 113**, pp. 61-68, 1991

11. I. Baumann, R. Brinkmann, M. Dinand, W. Sohler, and S. Westenhöfer, "Ti:Er:$LiNbO_3$ Waveguide Laser of Optimized Efficiency", IEEE J. Quantum Electron., **Vol. 32** (9), pp. 1695-1706, 1996

12. results achieved in the European RACE-project EDIOLL (R2013), unpublished

13. R. Brinkmann, W. Sohler and H. Suche: "Continuous-Wave Erbium-Diffused $LiNbO_3$ Waveguide-Laser", Electron. Lett., **Vol. 27** (5), pp. 415-416, 1991

14. P. Becker, R. Brinkmann, M. Dinand, W. Sohler, and H. Suche: "Er-diffused Ti: $LiNbO_3$ waveguide laser of 1562 and 1576nm emission wavelengths", Appl. Phys. Lett., **Vol. 61** (11), pp. 1257-1259, 1992

15. Suche, I. Baumann, D. Hiller, and W. Sohler, "Modelocked Er:Ti:$LiNbO_3$-waveguide laser", Electron. Lett. **Vol. 29** (12), pp. 1111-1112, 1993

16. Suche, R. Wessel, S. Westenhöfer, W. Sohler, S. Bosso, C. Carmannini, and R. Corsini, "Harmonically Modelocked Ti:Er:$LiNbO_3$-Waveguide Laser", Opt. Lett., **Vol. 20** (6), pp. 596-598, 1995

17.K. W. Cheung, S. C. Liew, C. N. Lo, D. A. Smith, J. E. Baran, and J. J. Johnson: "Simultaneous five-wavelength filtering at 2.2nm separation using acoustooptic tunable filter with subcarrier detection," Electron. Lett., **Vol. 25**, pp. 636-637, 1989

18.Brinkmann, M. Dinand, I. Baumann, Ch. Harizi, W. Sohler, and H. Suche: "Acoustically tunable wavelength filter with gain", Phot. Techn. Lett., **Vol. 6** (4), pp. 519-521, 1994

19.H. Herrmann, P. Müller-Reich, R. Reimann, R. Ricken, H. Seibert, and W. Sohler: "Integrated Optical, TE- and TM-Pass Acoustically Tunable, Double-Stage Wavelength Filters in $LiNbO_3$", Electron. Lett., **Vol: 28** (7), pp. 642-643, 1992

20.I. Baumann, D. Johlen, W. Sohler, H. Suche, and F. Tian: "Acoustically tunable Ti:Er: $LiNbO_3$-waveguide laser", in Proc. 20th European Conference on Optical Communication (ECOC '94), Florence, Italy, 1994, **Vol. 4**: Post Deadline Papers, pp. 99-102

21.E. Lallier, J. P. Pocholle, M. Papuchon, M. de Micheli, M. J. Li, Q. He, C. Grezes-Besset, "Integrated Nd:MgO:$LiNbO_3$ FM mode locked-waveguide laser", Electron. Lett. **Vol. 27** (11), pp. 936-937, 1991

22.Suche, D. Hiller, I. Baumann, and W. Sohler, "Integrated Optical Spectrum Analyzer with Internal Gain", IEEE Photon. Technol. Lett., **Vol. 7** (5), pp. 505-507, 1995

23.I. Baumann, S. Bosso, R. Brinkmann, R. Corsini, M. Dinand, A. Greiner, K. Schäfer, J. Söchtig, W. Sohler, H. Suche and R. Wessel, " Er-Doped Integrated Optical Devices in $LiNbO_3$", accepted for publication in IEEE J. Selected Topics in Quantum Electron.

24.J. Söchtig, R. Gross, I. Baumann, W. Sohler, H. Schütz, and R. Widmer: "DBR waveguide laser in erbium-diffusion-doped $LiNbO_3$", Electron. Lett., **Vol. 31** (7), pp. 551-552, 1995

25.J. Söchtig, H. Schütz, R. Widmer, R. Lehmann, and R. Gross:"Grating reflectors for erbium-doped lithium niobate waveguide lasers", Proc. SPIE Conf. ``Nanofabrication and Device Integration", **Vol. 2213**, pp. 98-107, 1994

26.J. Söchtig, H. Schütz, R. Widmer, R. Corsini, D. Hiller, C. Carmannini, G. Consonni, S. Bosso, and L. Gobbi: "Monolithically integrated DBR waveguide laser and intensity modulator in erbium doped $LiNbO_3$", Electron. Lett., **Vol. 32** (10), pp. 899-900, 1996

27.F. Tian, R. Ricken, S. Schmid, and W. Sohler: "Integrated Acousto-Optical Heterodyne Interferometer in $LiNbO_3$", in "Laser in der Technik", Proc. Congress Laser '93, Munich, June 1993, W. Waidlich (ed.), Springer Verlag 1993, pp. 725-728